

# Nanotaper mode converter based on silicon pillar waveguide

Huaxiang Yi (易华祥)<sup>1</sup>, Yang Zhu (祝阳)<sup>1</sup>, and Zhiping Zhou (周治平)<sup>2,3\*</sup>

<sup>1</sup>Wuhan National Laboratory for Optoelectronics, College of Science and Engineering, Huazhong University of Science and Technology, Wuhan 430074

<sup>2</sup>State Key Laboratory on Advanced Optical Communication Systems and Networks, Peking University, Beijing 100871

<sup>3</sup>School of Electrical and Computer Engineering, Georgia Institute of Technology, Atlanta, Georgia 30332, USA

\*E-mail: zjzhou@pku.edu.cn

Received December 15, 2008

A two-dimensional (2D) optimized nanotaper mode converter is presented and analyzed using the finite-difference time-domain (FDTD) method. It can convert the mode size in a silicon pillar waveguide (PWG) from  $4\ \mu\text{m}$  to  $1\ \mu\text{m}$  over a length of  $7\ \mu\text{m}$  and achieve a transmission efficiency of 83.6% at a wavelength of  $1.55\ \mu\text{m}$ . The dual directional mode conversion of the nanotaper and its ability to perform mode compression and expansion are also demonstrated. The broadband with high transmittance is satisfied in this structure. Using this silicon-based nanotaper, mode conversion between integrated photonic devices can be more compact and efficient.

OCIS codes: 230.3990, 230.7370.

doi: 10.3788/COL20090704.0312.

Pillar waveguides (PWGs) are periodic dielectric structures made by aligning a series of dielectric cylinders in air. They can be used to control the flow of light at the submicron scale<sup>[1]</sup> by exploiting the properties of total internal reflection and interference exhibited by the forward and backward waves traveling along the waveguide. PWGs are also able to manipulate the dispersion of the guided mode using the interference of the propagation waves. Unlike photonic band gap (PBG) crystal waveguides, PWGs require little periodic configuration in the transverse dimension, making them more compact for optical integrated circuits<sup>[2–5]</sup>.

Due to the advancement in fabrication technology for photonic integration, submicron waveguide devices have been rapidly developed in recent years. In these devices, the mode mismatch from the different light field sizes will cause much loss during the transmission, especially between light source and single mode waveguide. In order to reduce the loss, novel structures have been designed to act as converters between the large scale mode and the small scale mode. A taper has been utilized to couple and convert the large input mode to the small scale waveguide mode<sup>[6,7]</sup>. The problem with this is that the high convert efficiency demands a long length of taper, which limits the compactness of the devices. Photonic crystal has also been applied to form a taper configuration converting the mode size in the advantage of the ultra-compact and flexible configuration<sup>[8]</sup>. However, the lateral periods in waveguide limit the size of the taper. In this letter, a silicon nanotaper consisting of two-dimensional (2D) PWGs is proposed to reduce the scale of a nano mode converter with high efficiency. Due to its flexibility in being able to confine different mode dimensions, it can be easily used to perform mode conversion in an ultra-compact fashion<sup>[9,10]</sup>. An optimized nanotaper which can convert the mode size from  $4\ \mu\text{m}$  to  $1\ \mu\text{m}$  over a length of less than  $10\ \mu\text{m}$  is obtained. The

dual directional mode conversion of the nanotaper and wide bandwidth are satisfied. Mode conversion between integrated photonic devices can be realized efficiently in such an ultra-compact silicon-based nanotaper.

The proposed silicon PWG nanotaper structure consists of a sequence of pillars with gradually increasing radii aligned in air along the waveguide. By gradually varying the pillar radius, the PWG can be made to work as an index guiding structure for mode conversion. To compress the propagation mode, the proposed nanotaper is designed as a reverse spot size converter with smaller pillars at the input port and larger ones at the output port, as shown in Fig. 1, which can provide compact solution. The radii of the pillars increase gradually, assuming that  $d$  is the difference in radii among neighboring pillars and  $a$  is the period of the pillars.

When a mode of large field size is coupled into the nanotaper, the mode begins to convert along the taper. At the input port of the nanotaper, the input mode is weakly confined by the small pillar with its low effective reflection index<sup>[7]</sup>. As a result, any coupling mode loss caused by reflection is reduced. The pillar radius is then increased along the waveguide while maintaining a constant radius difference. The interference of waves among the pillars becomes stronger, leading to an enhanced mode confinement as discussed above. Such strong mode confinement compresses the mode dimension to a smaller scale. In this structure, the compression ability highly relies on the interference and mode confinement within the PWG, which is determined by the period and radius

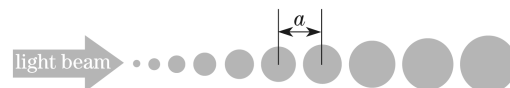


Fig. 1. Schematic of PWG nanotaper converter. The difference in radius between neighboring pillars is  $d$  and the period of the pillars is  $a$ .

variation of the nanotaper.

Our simulations were performed using the finite-difference time-domain (FDTD) method, with the perfectly matched layer boundary condition being specially chosen to reduce reflection. Since the 2D and three-dimensional (3D) cases in PWG have similar transmission characteristics, in FDTD simulation, we took the 2D condition to discuss the conversion performance<sup>[10]</sup>. Only TM mode was considered in this study, as in Refs. [2, 4]. The propagation wavelength was 1.55  $\mu\text{m}$ . The input mode was a Gaussian-shaped continuous wave with a mode size of 4  $\mu\text{m}$  as large as coupled from a lensed fiber at tip, while the target mode size was 1  $\mu\text{m}$  for a single mode waveguide. The output field power was monitored by an output detector. The effective indices of pillars and background are 3 and 1 according to the silicon-on-insulator slab with 300-nm silicon core and air, respectively.

The nanotaper structure used in our simulation is shown in Fig. 1. The mode compression transmission efficiency from the optical fiber to the sub-micron waveguide was calculated. The simulation results are presented in Fig. 2. In the nanotaper, from the light input port at the top, the propagation mode confinement was gradually improved, leading to a subsequent reduction in the mode size from 4  $\mu\text{m}$  to less than 1  $\mu\text{m}$ . We obtained a transmission efficiency of more than 86% and completed the mode conversion over a length of approximately 13  $\mu\text{m}$ . When changing the size of input optical field from 1  $\mu\text{m}$  to 8  $\mu\text{m}$ , the PWG taper is also able to compress the mode size to around 1  $\mu\text{m}$ . However, transmission efficiency higher than 80% can only be obtained with the input mode size ranging from 3 to 5  $\mu\text{m}$ . The main loss comes from the oscillation of light modes among pillars. There is a leaky when mode is not contained in the high index structures. However, the oscillations force the mode to be compressed high efficiently by the distribution of the pillars.

To study the influence of the period  $a$  on the coupling transmission efficiency, the same parameters were used in the simulation and only the period  $a$  was changed. The simulation results are shown in Fig. 3. With  $a$  being the only variable and the number of pillars kept constant, the transmission spectrum and length of the nanotaper as functions of the period are shown in Fig. 3. It can be seen that a larger period leads to a weaker interference, which reduces the transmission of the PWG

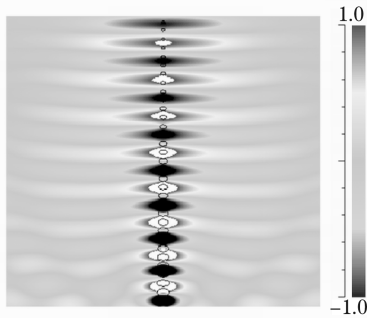


Fig. 2. Propagation mode in the PWG nanotaper for mode compression. The simulation wavelength is 1.55  $\mu\text{m}$  for TM polarization.

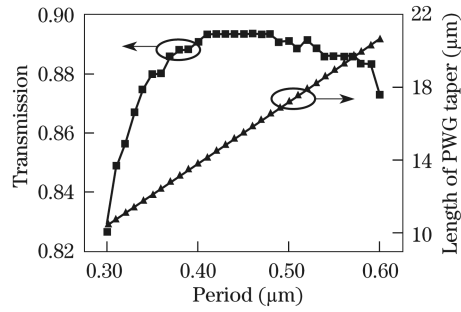


Fig. 3. Transmission and length of the PWG taper versus period.

taper, while a smaller period leads to overlapping of the pillars, which also reduces the transmission efficiency. We conclude that setting a suitable pillar period can reduce the length of the taper and enhance the conversion transmission.

Consider now the influence of the radius difference  $d$  on the transmission. It is designated that the sizes of the pillars at the input and output ports always ensure a high coupling efficiency and the target conversion mode scale. To simulate the effect of various  $d$ , the radii of the first and last pillars and period  $a$  were kept constant. As the radius difference  $d$  varied, both the number of pillars and length of the nanotaper changed. The changes in the transmission spectrum and number of pillars as functions of  $d$  are plotted in Fig. 4. It can be seen that a smaller  $d$  leads to a longer taper with a higher degree of conversion loss, while a larger  $d$  leads to dramatic changes along the waveguide, which also reduces the transmission efficiency. Optimizing  $d$  can balance the length and transmission efficiency of the PWG taper.

The above discussion indicates that the optimal structure for the proposed nanotaper is obtained at an ultra-compact scale. The optimized result is that a 7- $\mu\text{m}$ -long nanotaper converts the mode dimension from 4  $\mu\text{m}$  to less than 1  $\mu\text{m}$  with a transmission efficiency as high as 83.6% at 1.55- $\mu\text{m}$  wavelength.

Reverse mode conversion performs equally well. In the reverse mode conversion, the pillar radius along the nanotaper decreases, so does the confinement of the propagation mode. As a result, the mode dimension increases to the point where it matches the mode of the optical lensed fiber.

When the nanotaper is used for mode expansion, the input light mode diameter is 1  $\mu\text{m}$  coupled from a sub-micron waveguide at the butt, while the target mode size is 4  $\mu\text{m}$ . In simulating mode expansion, the light input port was at the top. Along the PWG, the propagation mode

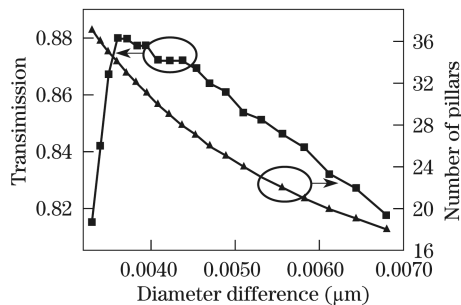


Fig. 4. Transmission and number of pillars in the PWG taper versus radius difference.

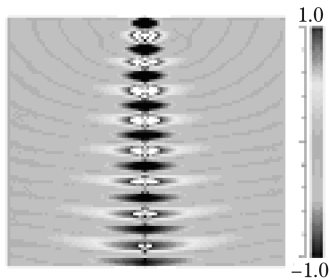


Fig. 5. Propagation mode in the PWG nanotaper for mode expansion. The simulation wavelength is  $1.55 \mu\text{m}$  for TM polarization.

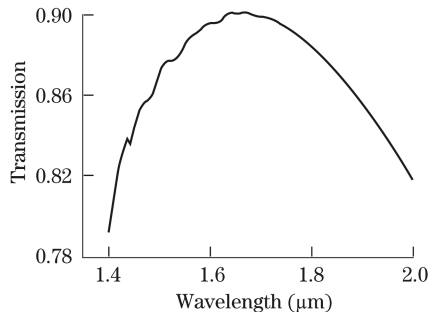


Fig. 6. Nanotaper with a bandwidth larger than  $380 \text{ nm}$  around  $1.55 \mu\text{m}$  and more than 86% mode conversion efficiency.

became deconfined and mode conversion from  $1 \mu\text{m}$  to approximately  $4 \mu\text{m}$  was obtained. Figure 5 shows that mode expansion occurs, with the transmission efficiency reaching almost 81%. The reason of the two transmission differences is that the input coupling effective index is larger in expansion, which leads to more reflection loss during the conversion. In this reverse process, the nanotaper has two kinds of conversion characteristics during coupling and exhibits high transmission.

Additional simulations were carried out to determine the bandwidth of the novel structure. Regarding bandwidth, by changing the coupling wavelength of the nanotaper we demonstrated that the PWG nanotaper had

a wide bandwidth of over  $380 \text{ nm}$ , with more than 86% mode conversion efficiency, as shown in Fig. 6.

In conclusion, we propose a silicon-based PWG nanotaper which is capable of realizing high-efficiency mode conversion over a short length with a broad bandwidth. The interference mechanism of the PWG enables the nanotaper to operate at low loss and an ultra-compact scale. By further optimizing the PWG configuration, we believe that this nanotaper can be a very promising compact device for mode conversion in integrated photonic applications.

This work was partially supported by the National Natural Science Foundation of China (Nos. 60578048 and 60706013), the National Basic Research Program of China (No. 2006CB708310), and the Creative Foundation of Wuhan National Laboratory for Optoelectronics (No. P080003).

## References

1. S. Fan, J. N. Winn, A. Devenyi, J. C. Chen, R. D. Meade, and J. D. Joannopoulos, *J. Opt. Soc. Am. B* **12**, 1267 (1995).
2. P.-G. Luan and K.-D. Chang, *Opt. Express* **15**, 4536 (2007).
3. W. Huang, Y. Zhang, and B. Li, *Opt. Express* **16**, 1600 (2008).
4. D.-S. Gao, R. Hao, and Z.-P. Zhou, *Chin. Phys. Lett.* **24**, 3172 (2007).
5. Q. Shi, X. Lin, X. Cai, and N. Zhao, *Acta Opt. Sin.* (in Chinese) **27**, 706 (2007).
6. I. Moerman, P. P. Van Daele, and P. M. Demeester, *IEEE J. Sel. Top. Quantum Electron.* **3**, 1308 (1997).
7. V. R. Almeida, R. R. Panepucci, and M. Lipson, *Opt. Lett.* **28**, 1302 (2003).
8. E. H. Khoo, A. Q. Liu, and J. H. Wu, *Opt. Express* **13**, 7748 (2005).
9. P.-G. Luan and K.-D. Chang, *Opt. Express* **14**, 3263 (2006).
10. D. N. Chigrin, S. V. Zhukovsky, A. V. Lavrinenko, and J. Kroha, *Phys. Stat. Sol. (a)* **204**, 3647 (2007).